Calibration of Pathogenicity Due to Variant-Induced Leaky Splicing Defects by Using BRCA2 Exon 3 as a Model System

Hélène Tubeuf, Sandrine M Caputo, Teresa Sullivan, Julie Rondeaux, Sophie Krieger, Virginie Caux-Moncoutier, Julie Hauchard, Gaïa Castelain, Alice Fiévet, Laëtitia Meulemans, et al.

Calibration of Pathogenicity Due to Variant-Induced Leaky Splicing Defects by Using *BRCA2* Exon 3 as a Model System

Hélène Tubeuf[1,2], Sandrine M. Caputo[3,4], Teresa Sullivan[5], Julie Rondeaux[1], Sophie Krieger[1,6], Virginie Caux-Moncoutier[3,4], Julie Hauchard[1], Gaia Castelain[1], Alice Fiévet[3,7,8], Laëtitia Meulemans[1], Françoise Révillion[9], Mélanie Léoné[10], Nadia Boutry-Kryza[10], Capucine Delnatte[11], Marine Guillaud-Bataille[8], Linda Cleveland[5], Susan Reid[5], Eileen Southon[5], Omar Soukarieh[1], Aurélie Drouet[1], Daniela Di Giacomo[1], Myriam Vezain[1], Françoise Bonnet-Dorion[12], Violaine Bourdon[13], Hélène Larbre[14], Danièle Muller[15], Pascal Pujol[16], Fátima Vaz[17], Séverine Audebert-Bellanger[18], Chrystelle Colas[3,4], Laurence Venat-Bouvet[19], Angela R. Solano[20], Dominique Stoppa-Lyonnet[3,7], Claude Houdayer[1,21], Thierry Frebourg[1,21], Pascaline Gaildrat[1], Shyam K. Sharan[5], and Alexandra Martins[1]

ABSTRACT

BRCA2 is a clinically actionable gene implicated in breast and ovarian cancer predisposition that has become a high priority target for improving the classification of variants of unknown significance (VUS). Among all *BRCA2* VUS, those causing partial/leaky splicing defects are the most challenging to classify because the minimal level of full-length (FL) transcripts required for normal function remains to be established. Here, we explored *BRCA2* exon 3 (*BRCA2*e3) as a model for calibrating variant-induced spliceogenicity and estimating thresholds for *BRCA2* haploinsufficiency. *In silico* predictions, minigene splicing assays, patients' RNA analyses, a mouse embryonic stem cell (mESC) complementation assay and retrieval of patient-related information were combined to determine the minimal requirement of FL *BRCA2* transcripts. Of 100 *BRCA2*e3 variants tested in the minigene assay, 64 were found to be spliceogenic, causing mild to severe RNA defects. Splicing defects were also confirmed in patients' RNA when available. Analysis of a neutral leaky variant (c.231T>G) showed that a reduction of approximately 60% of FL *BRCA2* transcripts from a mutant allele does not cause any increase in cancer risk. Moreover, data obtained from mESCs suggest that variants causing a decline in FL *BRCA2* with approximately 30% of wild-type are not pathogenic, given that mESCs are fully viable and resistant to DNA-damaging agents in those conditions. In contrast, mESCs producing lower relative amounts of FL *BRCA2* exhibited either null or hypomorphic phenotypes. Overall, our findings are likely to have broader implications on the interpretation of *BRCA2* variants affecting the splicing pattern of other essential exons.

Significance: These findings demonstrate that *BRCA2* tumor suppressor function tolerates substantial reduction in full-length transcripts, helping to determine the pathogenicity of *BRCA2* leaky splicing variants, some of which may not increase cancer risk.

Introduction

Since the identification of *BRCA1* (MIM #113705) and *BRCA2* (MIM #600185) as major hereditary breast and ovarian cancer (HBOC) genes, mutation screening has led to the discovery of 20,000 unique germline *BRCA1* and *BRCA2* variants (1). In female carriers of pathogenic *BRCA1* and *BRCA2* variants, the cumulative risk by 80 years of age of developing breast cancer was estimated at 72% and 69% and that of developing ovarian cancer at 44% and 17%, respectively (2). Heterozygous *BRCA2* mutations also confer moderate risk to pancreatic and prostate cancers (3). Moreover, biallelic *BRCA2* mutations are causative of Fanconi anemia (FA) where one allele is often hypomorphic (4). Today, one of the most important bottlenecks in HBOC diagnosis is the high fraction of variants of unknown

[1]Inserm U1245, UNIROUEN, Normandie University, Normandy Centre for Genomic and Personalized Medicine, Rouen, France. [2]Interactive Biosoftware, Rouen, France. [3]Department of Genetics, Institut Curie, Paris, France. [4]PSL Research University, Paris, France. [5]Mouse Cancer Genetics Program, Center for Cancer Research, National Cancer Institute, Frederick, Maryland. [6]Laboratory of Cancer Biology and Genetics, Centre François Baclesse, Caen, France - Normandie University, UNICAEN, Caen, France. [7]INSERM U830, University Paris Descartes, Paris, France. [8]Service Génétique des Tumeurs, Gustave Roussy, Villejuif, France. [9]Unit of Human Molecular Oncology, Centre Oscar Lambret, Lille, France. [10]Hospices Civils de Lyon, Bron, France. [11]Department of Genetics, Nantes University Hospital, Nantes, France. [12]Inserm U1218, Department of Genetics, Institut Bergonié, Bordeaux, France. [13]Department of Genetics, Institut Paoli-Calmettes, Marseille, France. [14]Laboratoire d'Oncogénétique Moléculaire, Institut Godinot, Reims, France. [15]Unité d'Oncogénétique, Centre Paul Strauss, Strasbourg, France. [16]Unité d'Oncogénétique, CHU Arnaud de Villeneuve, Montpellier, France. [17]Breast Cancer Risk Evaluation Clinic, Portuguese Institute of Oncology of Lisbon, Lisbon, Portugal. [18]Département de Génétique et Biologie de la Reproduction, CHU Morvan, Brest, France. [19]Service Oncologie, CHU Dupuytren, Limoges, France. [20]Genotipificacion y Cancer Hereditario, Departmento de Analisis Clinicos, Centro de Educacion Medica e Investigaciones Clinicas (CEMIC), Ciudad Autonoma de Buenos Aires, Argentina. [21]Department of Genetics, University Hospital, Normandy Centre for Genomic and Personalized Medicine, Rouen, France.

Note: Supplementary data for this article are available at Cancer Research Online (http://cancerres.aacrjournals.org/).

Corresponding Author: Alexandra Martins, Inserm U1245, UFR de Médecine et Pharmacie, 22 Bvd Gambetta, CS 76183, 76183 Rouen Cedex 1, France. Phone: 33-2-35-14-83-14; E-mail: alexandra.martins@univ-rouen.fr

Cancer Res 2020;80:3593–605

doi: 10.1158/0008-5472.CAN-20-0895

significance (VUS) detected in the *BRCA* genes, estimated at approximately 50% of the detected variants (5–9). Carriers of VUS and their relatives cannot benefit from cancer-risk-reducing strategies, such as increased surveillance and prophylactic surgery, or from targeted therapies. VUS are generally typified by missense changes, but also include synonymous substitutions, small in-frame insertions and deletions as well as intronic variants, all of which can potentially affect pre-mRNA splicing (10). A significant number of *BRCA* VUS has been shown to induce RNA splicing defects (11). Splicing defects that lead to the exclusive production of aberrant transcripts carrying a premature termination codon (PTC) or of in-frame deletions disrupting known functional domain(s) (12) are regarded as pathogenic. In contrast, the biological consequences of variants that lead to partial/leaky splicing defects [i.e., that still produce a certain level of full-length (FL) reference transcripts] remain unknown. In this respect, variants affecting the in-frame alternatively spliced *BRCA2* exon 3 (*BRCA2*e3) are particularly challenging to interpret.

*BRCA2*e3 encodes an essential bipartite region comprised of (i) a transactivation core that interacts with EMSY, and (ii) a PALB2-interaction domain that allows the recruitment of BRCA2 to the site of double stand breaks (DSB) to mediate homologous recombination (HR; Supplementary Fig. S1A; refs. 13, 14). Recently, it was demonstrated that variants that trigger total skipping of BRCA2e3 (leading to a 249-nucleotide in-frame deletion, Δ3; Supplementary Fig. S1B), such as c.316+5G>C, confer high-risk of developing *BRCA2*-associated cancers (12). In contrast, the biological impact of variants causing partial *BRCA2*e3 skipping remains unknown and their contribution to *BRCA2* haploinsufficiency and pathogenicity is not yet established. Indeed, the minimal level of full-length transcripts that can provide sufficient *BRCA2* function is still unknown. A low proportion of naturally occurring alternatively spliced transcripts lacking *BRCA2*e3 (Δ3∼1%–3%) has been detected in normal tissues, including blood, mammary glands, and prostate tissues (15–18). Furthermore, despite causing increased levels of Δ3 transcripts (estimated at ∼20% in blood-derived samples), c.68-7T>A was recently found to be a nonpathogenic variant as it was not associated with increased risk of breast cancer (posterior probability of 7.44×10^{-115}; ref. 19). Here, we hypothesized that *BRCA2*e3 variants with partial effects on splicing, though stronger than c.68-7T>A, would confer minimal to severe reduction in *BRCA2* function, depending on the severity of exon 3 skipping. These variants could thus be associated with varying degrees of cancer susceptibility.

We therefore investigated the impact of 100 variants on *BRCA2*e3 splicing by utilizing both *in silico* tools and functional assays. The biological consequences of seven noncoding variants (intronic or synonymous) that cause gradual increase of *BRCA2*e3 skipping were then assessed in a mouse embryonic stem cell (mESC)-based complementation assay. In addition, we collected patient-related data for these variants. We conclude that *BRCA2* tumor suppressor activity may tolerate substantial reduction in the level of full-length transcripts, a finding that could contribute to improve *BRCA* variant classification guidelines.

Materials and Methods

Variant selection

To calibrate the potential spliceogenicity of *BRCA2*e3 variants, we started by focusing on 74 translationally silent/noncoding variants (intronic or synonymous), most of which were bioinformatically predicted to induce *BRCA2*e3 splicing defects (Supplementary Fig. S2; Supplementary Table S1). These included 61 noncoding variants that were expected to affect *BRCA2*e3 splicing by either weakening the strength of 3′ and 5′ splice sites (3′ss and 5′ss; $n = 21$, Supplementary Fig. S3A and S3B) or by disrupting putative splicing regulatory elements (SRE; $n = 40$, Supplementary Fig. S4). Bioinformatics predictions of variant-induced alterations of 3′ss and 5′ss strength were performed with MaxEntScan (MES) and SpliceSiteFinder-like (SSFL), interrogated by using either Alamut Batch v1.9 or Alamut Visual v2.11 integrated software tools (Interactive Biosoftware, http://www.interactive-biosoftware.com), as well as SPiCE (RRID: SCR_016603, https://sourceforge.net/projects/spicev2-1/) (20). Predictions of variant-induced SRE alterations were obtained with four SRE-predictors, namely: QUEPASA (21, 22) and HEXplorer (23), for which the ΔtESRseq and ΔHZ_{EI} scores, respectively, were calculated with the Alamut Batch prototype tool version 1.5.2 (ESRseq; http://www.interactive-biosoftware.com) as well as SPANR (24) and HAL (25), for which Δψ scores were retrieved from the corresponding online interfaces (http://tools.genes.toronto.edu and http://splicing.cs.washington.edu/SE, respectively). Variants were selected based on the "at least three" rule, that is, we considered that the most probable spliceogenic variants were those predicted as such by at least three SRE predictors according to thresholds described in ref. 26 and shown in Supplementary Fig. S4. In addition and without prior knowledge of splicing predictions, we also integrated 13 noncoding *BRCA2* variants classified as VUS (or with discordant classifications in different databases), which had been detected in probands undergoing genetic testing in diagnostic laboratories from the French GGC-Unicancer network (Supplementary Fig. S2; Supplementary Table S1; Supplementary Note).

After the initial calibration experiments with the 74 noncoding variants, we also performed functional analyses with a set of missense variants ($n = 24$) identified in probands undergoing genetic counselling. Two pathogenic variants, c.92G>A (p.Trp31*) and c.145G>T (p.Glu49*), which were previously described as spliceogenic in minigene splicing assays (27, 28), were also retained as controls. Therefore, altogether, our collection included a total of 100 *BRCA2e3* variants.

Minigene splicing assays

To evaluate the impact on splicing of the 100 *BRCA2*e3 variants, we performed functional assays based on the comparative analysis of the splicing pattern of wild-type (WT) and mutant reporter minigenes. Minigenes were prepared by using the pCAS2 vector backbone as described previously (26, 29) and explained in Supplementary Materials and Methods.

Analysis of the *BRCA2* exon 3 splicing pattern in RNA samples from patients and control individuals

RNA samples from EBV-immortalized lymphoblastoid cell lines (LCL) or PAXgene-stabilized blood of healthy donors and patients were collected in collaboration with the GGC-Unicancer consortium (Supplementary Note). The splicing patterns of *BRCA2* transcripts expressed in LCL or PAXgene samples were analyzed by semiquantitative fluorescent RT-PCR (26 and 40 cycles, respectively), as further described in Supplementary Materials and Methods, with primers mapping to *BRCA2* exons 2 and 5 (Supplementary Table S2).

Allele-specific expression analysis

Allele-specific expression (ASE) of *BRCA2*e3-containing transcripts (FL) was measured by performing a quantitative primer extension assay (SNaPshot MultiplexKit, Applied Biosystems), as described previously (29), using specific primers targeting the variants of interest (Supplementary Table S2) and semiquantitative RT-PCR conditions further detailed in Supplementary Materials and Methods.

mESC-based complementation assay

To assess the functional impact of *BRCA2*e3 variants, we took advantage of a mESC-based assay (30, 31). Mouse ESC-expressing the human *BRCA2* gene (*hBRCA2*) carrying specific variants were generated as described previously (30, 31) with a few modifications as detailed in Supplementary Materials and Methods. After Cre-mediated deletion of the conditional mouse *Brca2* allele (*mBrca2*), we assessed cell survival and sensitivity to DNA-damaging agents, as described previously (30, 31). The splicing patterns of *BRCA2*e3 were analysed by semiquantitative fluorescent RT-PCR (24 cycles), as described for patient RNA.

Patient and family data

Genetic, clinical, familial, and tumoral data for patients carrying *BRCA2*e3 variants were collected in collaboration with the French GGC network and within the framework of the COsegregation of VARiants in the *BRCA1/2* and *PALB2* genes clinical trial (COVAR, Supplementary Note). The criteria for diagnostic variant screening of the *BRCA2* gene were applied according to the current French GGC recommendations and the French National Cancer Institute (INCa) guidelines. Informed written consent was obtained from all patients.

Consortia

Members of the French GGC network and of the COVAR (COsegregation of VARiants in the *BRCA1/2* and *PALB2* genes) group are listed in the Supplementary Note.

Results

Identification of variants affecting *BRCA2*e3 splicing by using a minigene splicing assay

To get a glimpse of *BRCA2e3* vulnerability to predicted splicing mutations and to calibrate the spliceogenicity of this exon, we started by evaluating the impact on splicing of 74 noncoding variants by performing a minigene assay (**Fig. 1A**). These variants, which map either to exon 3 or its flanking intronic regions, included 61 noncoding variants bioinformatically predicted to induce exon skipping (19 intronic, 2 synonymous but overlapping exon–intron junctions and 40 exonic synonymous variants; 26/61 being naturally occurring variants described in Human variation databases). We included 13 additional noncoding variants that were selected because they were either classified as VUS in BRCA-Share or had conflicting interpretations in other databases (4 intronic and 9 exonic synonymous; Supplementary Figs. S2–S4; Supplementary Table S1).

The minigene splicing assay, which was based on pCAS2-BRCA2e3-derived constructs (Supplementary Fig. S5), revealed that 52 out of the 74 variants (70%) altered the splicing pattern of *BRCA2*e3, whereas 22 of 74 remaining variants (30%) showed no major effect on splicing (**Fig. 1B**; Supplementary Table S1). More precisely, 51 variants induced *BRCA2*e3 skipping to different extents (6%–100% Δ3, i.e., 94%–0% FL) and 1 variant (c.68-1G>A) resulted in complete deletion of six nucleotides at the beginning of the exon, due to the creation of a new 3′ss (Supplementary Fig. S6). Because it causes a small in-frame deletion, the latter should now be considered a VUS instead of a likely pathogenic variant as currently indicated in ClinVar. We found that *in silico* analyses were generally useful for predicting variant-induced splicing alterations, but that not all predictions were correct (Supplementary Tables S1, S3–S5; Supplementary Figs. S7A, S7B, S8A–S8E and S9A–S9E). For instance, the naturally occurring c.231T>G synonymous VUS caused 31% Δ3 (69% FL), which is concordant with a previous experimental study (32), but disagrees with the SRE predictions (Supplementary Table S1). In sum, these data suggest that the regulation of *BRCA2e3* splicing is very plastic and allowed us to initiate a calibration of the variant-induced spliceogenicity of this exon. Indeed, we observed a spectrum of splicing alterations varying from mild (corresponding to a level of exon inclusion lower than WT, i.e., <99%, but ≥92%, a threshold defined by the effect of the neutral c.68-7T>A variant) to drastic (exon inclusion ≤5%, defined by the impact of the pathogenic c.316+5G>C variant; **Fig. 1B**). On the basis of this comparative analysis, we infer that the noncoding variants in our dataset that show levels of exon inclusion in the minigene assay equal or superior to c.68-7T>A are neutral, whereas those that lead to exon inclusion levels equal or inferior to c.316+5G>C are pathogenic. Seven VUS causing intermediate levels of exon inclusion (92%>FL>5%) were retained for further analysis because they illustrate the continuum of variant-induced FL transcript loss observed in the minigene assay and could eventually help in defining a Δ3 threshold for pathogenicity (c.165C>T, c.231T>G, c.68-8_68-7delinsAA, c.102A>G, c.316+6T>C, c.316+6T>A and c.316+6T>G, in increasing order of severity; **Fig. 1C**).

Confirmation of variant-induced spliceogenicity in RNA samples from patients with HBOC

To assess the physiologic relevance of the splicing defects revealed by the minigene assay, we analyzed the splicing pattern of *BRCA2*e3 in human-derived samples, either LCL or PAXgene-stabilized blood, obtained from control individuals and from four patients carrying *BRCA2*e3 variants (c.231T>G, c.68-8_68-7delinsAA, c.102A>G, and c.316+6T>C). No biological samples were available for carriers of c.165C>T, c.316+6T>A, and c.316+6T>G. Besides LCL and PAXgene samples from healthy individuals, two additional controls were used in this experiment: (i) a LCL from a patient harboring an unequivocal pathogenic Alu insertion in the middle of exon 3 (c.156_157insAlu) known to cause total exon skipping (33) and LCLs from four carriers of the neutral variant c.68-7T>A, known to lead to mild exon skipping (19). The biallelic splicing patterns of *BRCA2*e3 in patient biological samples were analyzed by semiquantitative RT-PCR, a common approach used in clinical settings (34), and compared with those generated from equivalent RNA samples of control individuals (**Fig. 2A** and **B**; Supplementary Table S1). In LCL and PAXgene samples from healthy controls, we detected the natural alternative splicing pattern of *BRCA2e3* with approximately 10% Δ3, whereas carriers of c.68-7T>A displayed approximately 25% Δ3. These splicing patterns are comparable with previous reports of approximately 3% Δ3 in LCL control samples and approximately 13% Δ3 in carriers of c.68-7T>A as determined by qRT-PCR (19). Importantly, heterozygous carriers of c.231T>G, c.68-8_68-7delinsAA, c.102A>G, and c.316+6T>C showed a decrease in the relative amount of FL transcripts due to an increase in Δ3 (75%–38% FL; i.e., 25%–62% Δ3). These relative levels of Δ3 were lower than that observed for c.156_157insAlu (FL = 30%, i.e., Δ3 = 70%), suggesting that these four variants are leaky not only in the minigene assay but also in patients' cells. Nevertheless, assuming a balanced biallelic expression of *BRCA2* and taking into account that WT alleles seem to contribute to approximately 10% Δ3, it was expected that the LCL carrying the heterozygous c.156_157insAlu variant would display approximately 55% Δ3, instead of 70% as detected. It is thus possible that our RT-PCR conditions slightly overestimate the level of Δ3 possibly due to a PCR bias favoring the amplification of the smaller Δ3 RT-PCR products

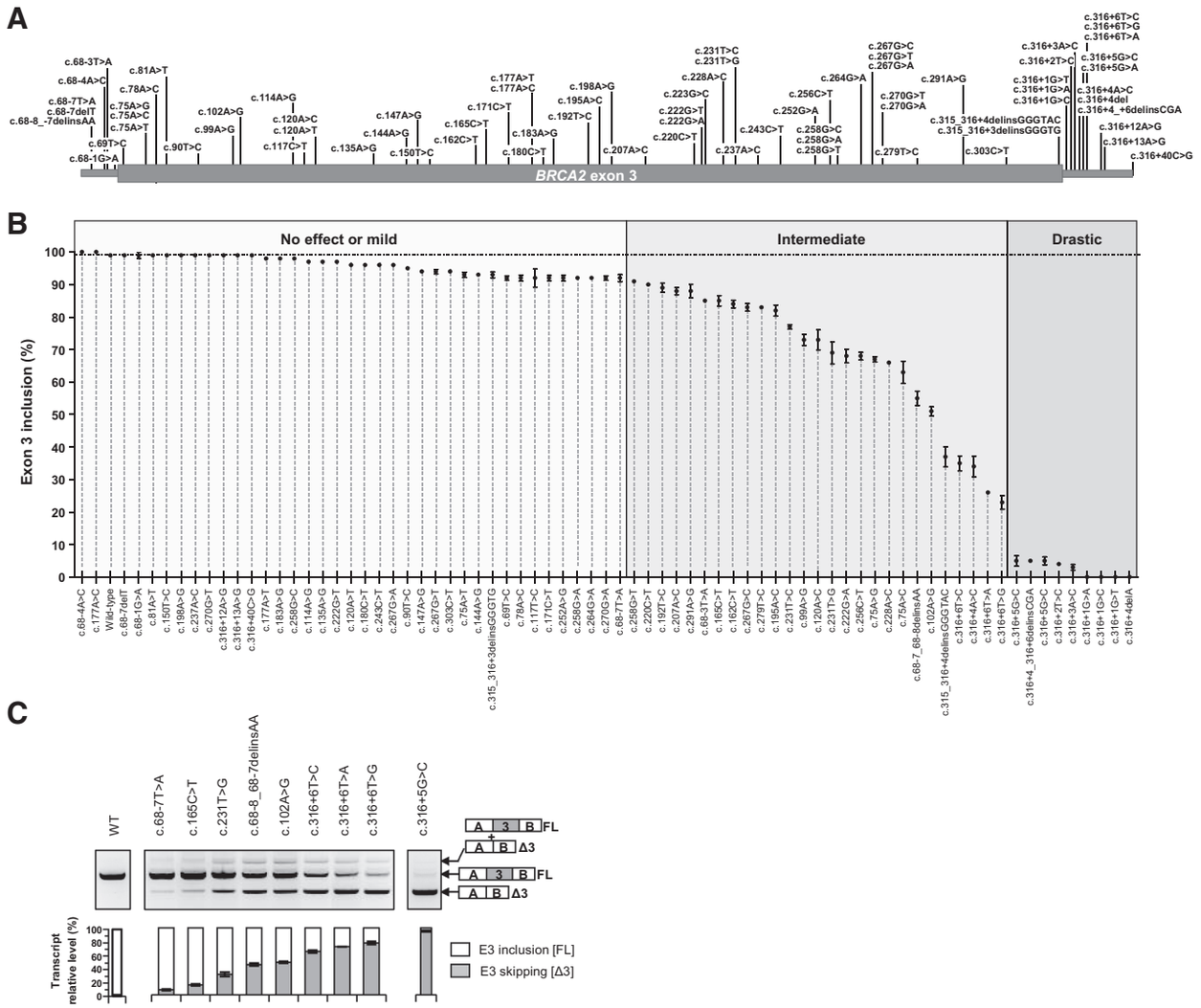

Figure 1.

Identification of *BRCA2* exon 3 spliceogenic variants among translationally silent genetic alterations by using a minigene splicing assay. **A,** Distribution of the 74 variants reported within or in the vicinity of *BRCA2* exon 3. The diagram shows the relative position and identity of each variant within *BRCA2*e3 and flanking intronic regions. **B,** Impact on splicing of noncoding *BRCA2* exon 3 variants. WT and mutant pCAS2-*BRCA2*-e3 minigene constructs were transiently expressed in HeLa cells. The splicing patterns of the RNA produced from the different minigenes were then analyzed by semiquantitative fluorescent RT-PCR, followed by capillary electrophoresis. Results represent the mean of relative exon 3 inclusion (% FL) of three independent transfection experiments. Error bars, SEM values. **C,** Splicing pattern of pCAS2-*BRCA2*e3 minigenes carrying selected variants that cause gradual increase in *BRCA2*e3 skipping. Top, the RT-PCR products separated on an agarose gel. Bottom, the relative quantification of the fluorescent RT-PCR products separated by capillary electrophoresis. Results represent the mean of three independent transfection experiments. Error bars, SEM values. The identities of the two RT-PCR products obtained, with (FL) or without (Δ3) exon 3, are indicated on the right. FL+Δ3 correspond to heteroduplexes containing the two products. E3, exon 3.

relative to FL. A similar impact on exon 3 splicing was observed by Colombo and colleagues but the effect was more exacerbated probably due to a higher number of PCR amplification cycles (19). Sequencing of the FL RT-PCR products of patients carrying the heterozygous c.231T>G variant showed the presence of both WT and mutant FL transcripts, with mutant FL transcripts appearing to be underrepresented as compared with WT, further suggesting that this variation cause partial splicing defects (Supplementary Fig. S10). These results obtained from patient-derived RNA samples are in agreement with the minigene data. Indeed, we observed a good correlation (R^2 = 0.9601, Supplementary Fig. S11A) between the levels of *BRCA2*e3 skipping evaluated in the monoallelic minigene-based assay and those assessed in RNA samples derived from patients carrying the same variants at the heterozygous state. Moreover, to better evaluate the contribution of WT and mutant alleles to the production of FL transcripts, we took advantage of the quantitative nature of the SNaPshot assay, which allows the measurement of ASE, i.e., the relative contribution of each allele to the production of RT-PCR products containing *BRCA2e3* (**Fig. 2C**). ASE analysis indicated that FL transcripts expressed from the mutant alleles were in fact present in cells of a patient carrying c.102A>G (53% of WT) and c.231T>G (56%, 62%, 65% or 108% of WT, depending on the

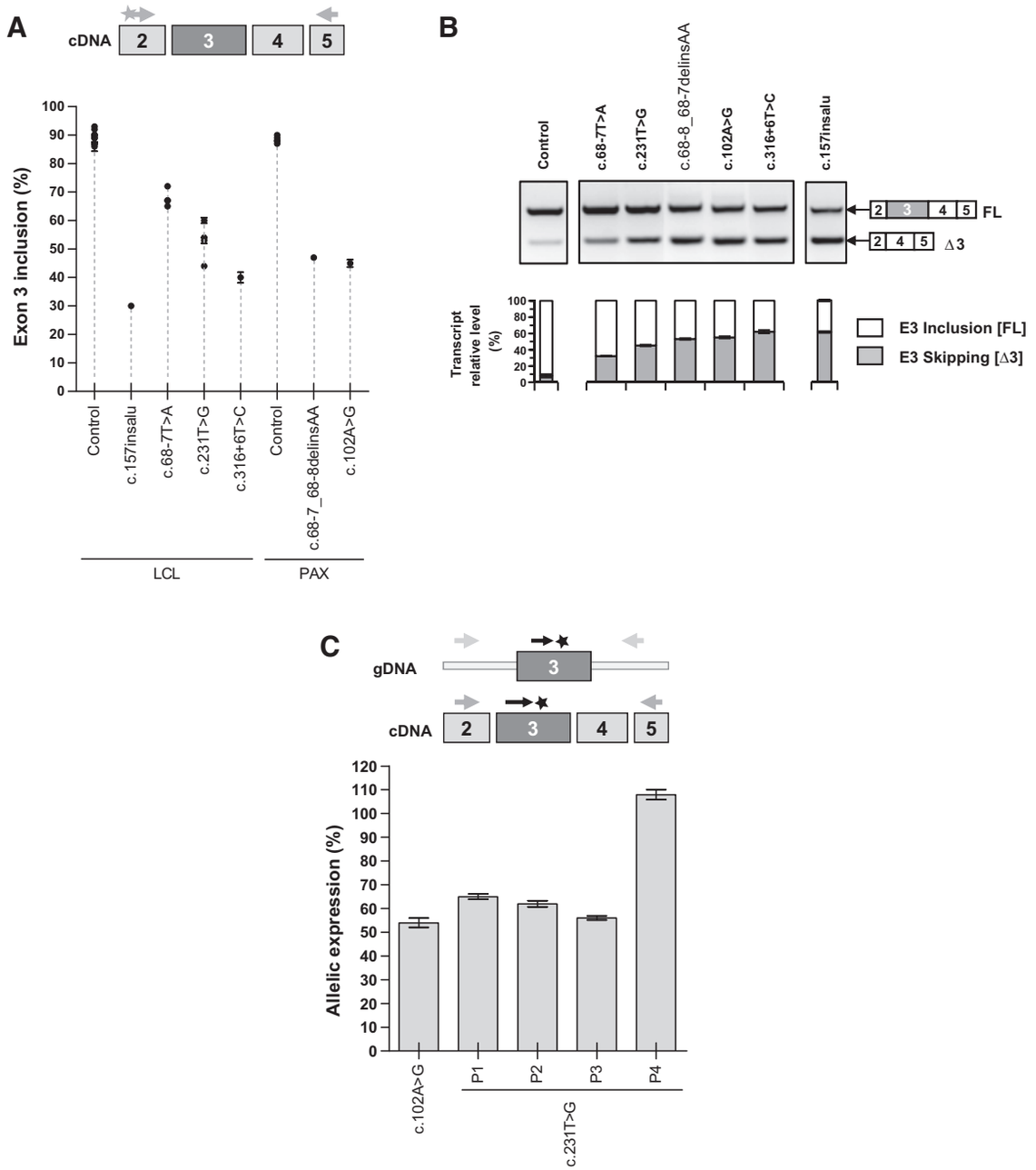

Figure 2.

BRCA2 exon 3 splicing patterns and allele-specific expression in patients carrying translationally silent variants. **A,** Alterations in the relative level of exon 3 inclusion caused by *BRCA2*e3 variants. The *BRCA2*e3 splicing patterns in patient-derived RNA samples were monitored by semiquantitative fluorescent RT-PCR by using forward and reverse primers located in exons 2 and 5, respectively, followed by capillary electrophoresis and compared with those from healthy donors (controls). The relative levels of exon inclusion (bottom) refer to the amount of full-length transcripts (FL; containing exon 3) relative to the total amount of transcripts (with and without exon 3) and are representative of three independent experiments. Error bars, SEM. **B,** Splicing pattern of *BRCA2*e3 variants shown in increasing order of spliceogenicity. Top, RT-PCR products separated on an agarose gel. Bottom, the relative quantification of the same products separated by capillary electrophoresis as described in **A**. Results represent the mean of three independent experiments and they all concern LCL RNA except for c.68-8_68-7delinsAA and c.102A>G that refer to PAXgene samples. Error bars, SEM values. The identities of the two RT-PCR products obtained, with (FL) or without (Δ3) exon 3, are indicated on the right. E3, exon 3. **C,** Allele-specific expression of transcripts including *BRCA2* exon 3 assessed by SNaPshot analysis. Genomic segment (gDNA) and complementary DNA (cDNA) containing *BRCA2*e3 were amplified in parallel using specific primers (gray arrows) and the SNaPshot quantitative primer extension assay was then performed with a variant-specific primer (black arrow) targeting the sequence immediately upstream the *BRCA2*e3 variant. Allele-specific expression, representing the relative contribution of the variant allele to the expression of full-length *BRCA2* transcripts as compared with WT (% of WT), was measured by normalization of the cDNA peak area ratio (variant/WT) to the corresponding gDNA peak area ratio (variant/WT). Results are representative of three independent experiments. Error bars, SEM values. P, patient.

patient). On the basis of the results of our minigene assays and RT-PCR analysis of patient RNA, we concluded that the observed allelic imbalances in FL transcripts are essentially due to variant-induced *BRCA2*e3 skipping and that the variants cause partial rather than total splicing defects. Surprisingly, we did not observe an allelic imbalance for one of the carriers of c.231T>G (108% of WT) despite an increase in Δ3 in patient biological material. Importantly, we found that this patient also harbors a pathogenic nonsense variation (*BRCA2* c.6515C>A, p.Ser2172*) *in trans* of c.231T>G. Most likely, the PTC introduced by the nonsense variation leads to nonsense-mediated decay of the transcripts expressed from this allele to a level similar to that of c.231T>G-induced exon skipping. Of note, we observed a correlation between the levels of *BRCA2e3* skipping evaluated in the minigene assay and the ASE results obtained with equivalent patient-derived RNA samples ($R^2 = 0.9417$; Supplementary Fig. S11B). We surmise from these results that the minigene assay is a good surrogate system to evaluate the spliceogenicity of *BRCA2e3* variants.

Functional characterization of *BRCA2*e3 spliceogenic variants in a mESC-based assay

In an attempt to uncover a RNA-related threshold for *BRCA2* haploinsufficiency, we evaluated the consequences of variant-induced *BRCA2e3* skipping in *BRCA2* function by performing a mESC-based complementation assay (**Fig. 3A**; Supplementary Fig. S12). Here, we tested seven variants: four intronic (c.68-8_68-7delinsAA, c.316+6T>A, c.316+6T>C, and c.316+6T>G) and three synonymous (c.102A>G, c.165C>T and c.231T>G). These variants were selected on the basis of four main reasons. First, they caused a gradual increase in Δ3 in the minigene assay. Second, they are all translationally silent, which avoids any potential confounding effect produced by coding changes. Third, they are clinically interesting given that all except one (c.316+6T>A) were identified in patients suspected of HBOC. And fourth, their pathogenicity is unknown. We also included c.68-7T>A and c.316+5G>C as controls because these spliceogenic variants have been unequivocally classified as neutral and pathogenic, respectively (12, 19).

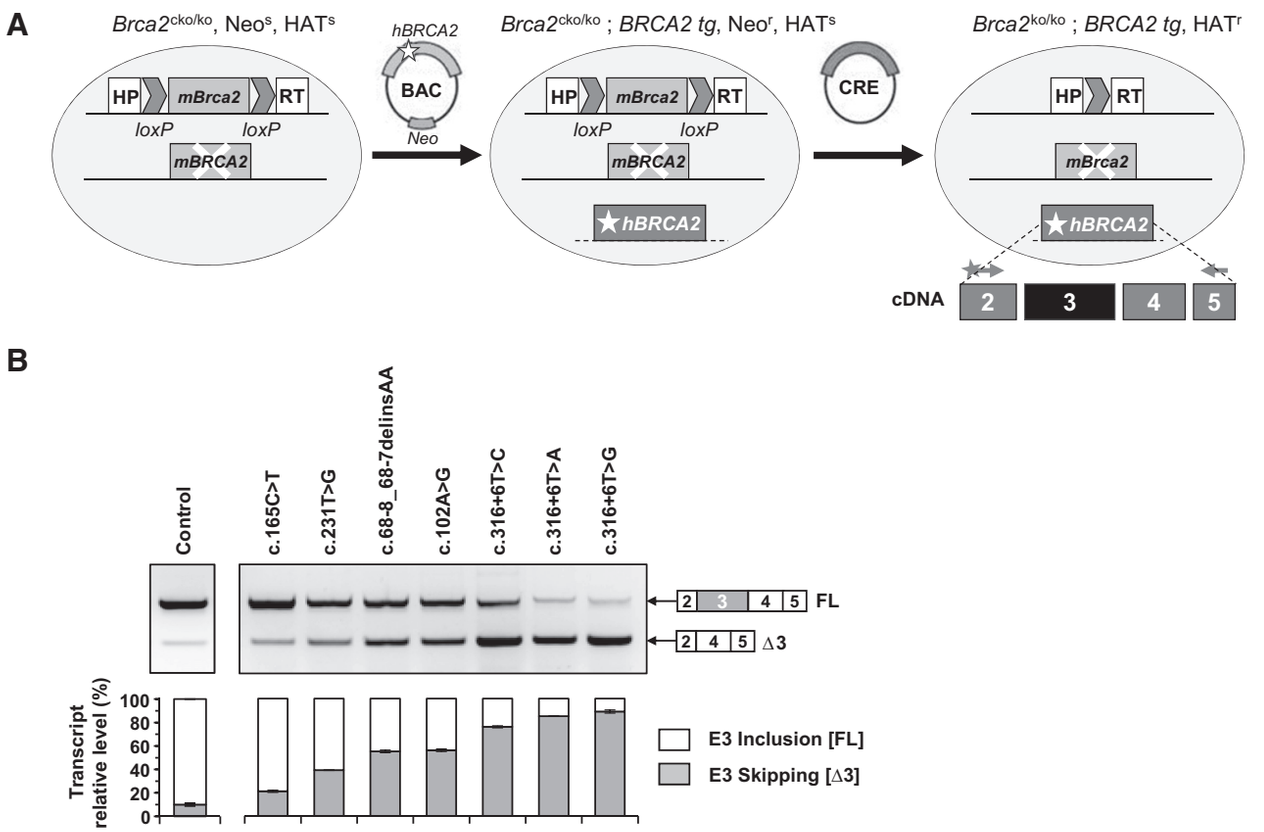

Figure 3.

Functional analysis of *BRCA2* translationally silent variants that cause gradual increase in exon 3 skipping by using a mouse embryonic stem cell (mESC)-based assay. **A,** Schematic representation of the mESC model used for the functional analysis of *BRCA2*e3 variants. PL2F7 mESCs with a conditional (*cko*) mouse *Brca2* allele (m*Brca2*) flanked with two *loxP* sites along with two halves (designated as HP and RT) of the human *HPRT1* minigene and a knockout (*ko*) of the second m*Brca2* allele were electroporated with BACs carrying human *BRCA2* (WT or variant *hBRCA2*). Resulting colonies were selected for further analysis after verification of h*BRCA2* expression by Western blot analysis (Supplementary Fig. S12). Then the conditional m*Brca2* allele was deleted by transient expression of Cre in the selected cells. Variants that could (fully or partially) complement BRCA2 deficiency resulted in HAT-resistant clones (Supplementary Fig. S13). These viable clones were used for other functional studies including sensitivity to DNA-damaging agents (Supplementary Fig. S14). *BRCA2*e3 splicing patterns in HAT-resistant mESC were monitored by semiquantitative fluorescent RT-PCR by using forward and reverse primers located in exons 2 and 5, respectively, followed by capillary electrophoresis. Results from mESC complementation assays are summarized in **Table 1**. **B,** RT-PCR analysis of the splicing pattern of mESC expressing *hBRCA2* variants. Top, the RT-PCR products separated on an agarose gel. Bottom, relative quantification of equivalent fluorescent RT-PCR products separated by capillary electrophoresis. Results represent the mean of three independent experiments. Error bars, SEM values. The identities of the two RT-PCR products obtained, with (FL) or without (Δ3) exon 3, are indicated on the right. E3, exon 3; P, patient.

Table 1. Summary of functional effects of *BRCA2*e3 variants analyzed in a mESC-based assay.

Nucleotide	Amino acid	Complementation[a]	Sensitivity[b]	Splicing (FL%)[c]		Classification[d]
				Detected	% WT	
WT	–	Yes	No	90	100	–
c.68-7T>A	p.?	Yes	No	nd	nd	Neutral
c.165C>T	p.(Asn55=)	Yes	No	79	88	Neutral
c.231T>G	p.(Thr77=)	Yes	No	61	68	Neutral
c.68-8_68-7delinsAA	p.?	Yes	No	45	50	Neutral
c.102A>G	p.(Glu34=)	Yes	No	44	49	Neutral
c.316+6T>C	p.?	Yes	No	24	27	Neutral
c.316+6T>A	p.?	Poor	Yes	15	17	VUS (intermediate)
c.316+6T>G	p.?	Poor	Yes	11	12	VUS (intermediate)
c.316+5G>C	p.?	No	n/a	n/a	n/a	Pathogenic
c.316G>A	p.Gly106Arg	Poor	Yes	25	28	VUS (intermediate)

Abbreviations: n/a, not applicable; nd, not determined; p?, variant of unknown protein consequences (non-coding but it may affect RNA splicing) as per HGVS nomenclature.

[a]Complementation phenotypes of *BRCA2*e3 variants based on viability of $Brca2^{ko/ko}$ mESCs expressing either WT or mutant *BRCA2* after deletion of the conditional allele (see also **Fig. 3**; Supplementary Fig. S13).

[b]Sensitivity of HAT-resistant mESCs (expressing either WT or mutant *hBRCA2*) to six DNA-damaging agents (olaparib, methyl methanesulfonate, mitomycin C, cisplatin, camptothecin, and ionizing radiation). Survival was measured by XTT assay and then compared with that of mESCs expressing wild-type *hBRCA2* (see also Supplementary Fig. S14).

[c]Relative quantification of splicing events in HAT-resistant mESCs expressing either WT or mutant *hBRCA2* was evaluated by semiquantitative fluorescent RT-PCR, followed by capillary electrophoresis. Results represent the mean of three independent experiments. Values relative to %WT were extrapolated from RT-PCR results displayed in the previous column (FL%) and assuming a similar *BRCA2* expression in the different mESCs clones.

[d]Suggested nucleotide variant classification based on the results of the mESC complementation assay.

We first tested the ability of the variants to rescue the cell lethality conferred by loss of *BRCA2* after loxP/Cre-mediated deletion of the endogenous conditional *mBrca2* allele (**Fig. 3A**; **Table 1**; Supplementary Fig. S13). The two loxP sites of the conditional *mBrca2* are flanked by two halves of human *HPRT* minigene, which allow selection of recombinant clones in the presence of HAT. We observed that mESCs expressing the c.316+5G>C pathogenic variation were unable to form HAT-resistant colonies, indicating that *BRCA2* function was severely impaired, a result that is in agreement with the deleterious nature of this variant (12). In contrast and as expected, the neutral variation c.68-7T>A (19) was able to fully complement the loss of endogenous *mBrca2*. Interestingly, the complementation phenotype of five of the seven VUS, namely c.165C>T, c.231T>G, c.102A>G, c.68-8_68-7delinsAA and c.316+6T>C, resembled that of the neutral variant. However, in the case of c.316+6T>A and c.316+6T>G (variants that had the most severe splicing defects in the minigene assay among the seven VUS of interest), we observed fewer HAT-resistant colonies as compared with WT-expressing cells, indicating that *BRCA2* function was compromised in these cells, resulting in incomplete/poor complementation (Supplementary Fig. S13).

Because *BRCA2* has an important role in the repair of DSBs, loss of its function renders cells vulnerable to compounds that introduce toxic DNA lesions (35). Therefore, we next tested the sensitivity of the HAT-resistant mESC to six DNA-damaging agents (cisplatin, mitomycin C, methyl methanesulfonate, olaparib, camptothecin, and γ-irradiation) by cell survival measurements (**Table 1**; Supplementary Fig. S14). As expected, c.68-7T>A-expressing cells exhibited no difference in sensitivity to various DNA-damaging agents as compared with WT-expressing cells. Similarly, mESC carrying either c.165C>T, c.231T>G, c.102A>G, c.68-8_68-7delinsAA, or c.316+6T>C did not exhibit hypersensitivity to any of the DNA-damaging agents, strongly supporting that they are fully functional and are likely to be neutral variants. In contrast, c.316+6T>A and c.316+6T>G are associated with a severe hypersensitivity to various DNA-damaging agents as compared with WT or to c.68-7T>A-expressing cells, strongly indicating an impairment in *BRCA2* function. We surmise that a reduction in FL transcripts down to 35% (as measured for the borderline c.316+6T>C variant in the minigene assay) is sufficient for *BRCA2* function, whereas a level equal to or lower than 26% FL (as measured for c.316+6T>A in the minigene assay) leads to *BRCA2* haploinsufficiency in mESCs. Moreover, a total loss-of-function was observed in mESCs when FL≤5% (as measured for c.316+5G>C in the minigene assay).

To validate the physiologic relevance of the mESC system for the evaluation of variant-induced *BRCA2*e3 splicing defects, we analyzed the splicing patterns of the different *BRCA2* variants in viable mESCs by semiquantitative RT-PCR. The WT *BRCA2* gene expressed in this system reproduced the alternative splicing of *BRCA2e3* (Δ3 = 10%, **Fig. 3B**) typically detected in normal human cells. Importantly, we confirmed that the five VUS that were fully functional in the mESC assay had increased levels of Δ3 representing a decrease in FL transcripts down to 27% of the WT *BRCA2* FL transcripts as extrapolated from the RT-PCR results. In contrast, c.316+6T>A and c.316+6T>G, which showed poor mESC-complementation, had even lower relative levels of FL transcripts (17% and 12%, respectively). These data suggests that the upper threshold for *BRCA2* haploinsufficiency in the mESCs lies between approximately 17% and approximately 27% FL and that for total loss-of-function the cutoff lies below 12% FL. The results of the mESC-derived RNA analysis were fully consistent with those obtained in the minigene assay not only in terms of whether or not a variant caused aberrant splicing but also in terms of the relative severity of the splicing defects ($R^2 = 0.9974$; Supplementary Fig. S15). Moreover, the results obtained in mESCs agree with those obtained with patient-derived samples, which highlights the physiologic pertinence of the mESC model to evaluate the consequences on splicing of *BRCA2*e3 variants. A biological classification of the selected variants based on the mESC complementation results is shown on **Table 1**.

Association of leaky *BRCA2* exon 3 variants with cancer risk

To gain insight into the clinical significance of leaky *BRCA2*e3 spliceogenic variants, we collected patient information for the seven

VUS analyzed in the mESC assay (Supplementary Table S6). Only one variant (c.231G>T) could be classified as neutral according to ACMG (36) and ENIGMA (37) guidelines given its: (i) high frequency in the African population (0.66%), (ii) the description of an homozygous individual in the general population; and (iii) the cooccurrence *in trans* with pathogenic *BRCA2* variants in HBOC patients without a FA phenotype. These data confirm that a decrease in FL transcripts from one *BRCA2* allele at least down to approximately 60% of WT (as determined for c.231G>T in the ASE analysis) is not associated with HBOC. Multifactorial likelihood analyses based on clinical, familial, and tumoral data from patients carrying four of the seven VUS (c.68-8_68-7delinsAA, c.102A>G, c.316G>A, and c.316+6T>C) were inconclusive, in part, because few families were accessible for analysis and no cosegregation information was available.

Functional impact of *BRCA2* missense VUS

Finally, we extended our minigene splicing analysis to 26 *BRCA2e3* coding variants (**Fig. 4A**) including all missense changes reported in the BRCA-Share database ($n = 23$), as well as one FA-associated missense variant (c.316G>A) and two previously described spliceogenic nonsense variants (c.92G>A and c.145G>T) (27, 28), the latter used as additional *BRCA2e3* spliceogenic controls. Of note, among the 24 missense variants, 21 were described as VUS (Supplementary Table S1). The minigene assay revealed that 12 out of the 26 variations tested (46%) altered the splicing pattern of *BRCA2*e3 relative to WT (**Fig. 4B**; Supplementary Table S1). More precisely, 11 variants increased *BRCA2*e3 skipping, including c.92G>A and c.145G>T as expected, and one variant (c.100G>A) caused two concomitant partial splicing defects, that is, skipping of *BRCA2*e3 and a 45-nucleotide in-frame deletion at the beginning of the exon caused by the creation of a new 3′ss (Supplementary Fig. S16). Given their positions within the exon, we suspect that c.316G>C and c.316G>A induce exon skipping by directly decreasing the strength of the 5′ss (Supplementary Fig. S7), whereas the remaining spliceogenic missense variants likely modify exonic SREs. Importantly, we confirmed that four of the variants (c.92G>A, c.145G>T, c.316G>A, and c.316G>C) are associated with a major relative increase of Δ3 in patients' RNA as compared with healthy controls (**Fig. 4C**). Moreover, ASE analysis revealed a reduction in FL transcripts expressed from the mutant alleles in these biological samples (50%–24% of WT, **Fig. 4C** and **D**). In contrast, the 14 remaining variants showed no effect on splicing in the minigene assay (**Fig. 4B**), including c.223G>C, a variant that is associated, in patient RNA, with a splicing pattern similar to that observed in control samples (**Fig. 4C**) and to an absence of *in vivo* allelic imbalance (**Fig. 4D**), which is consistent with the minigene results.

Our findings reiterate the importance of the minigene assay in assessing the impact on splicing of *BRCA2e3* variants. Moreover, they pinpoint c.316G>A (p.Gly106Arg) as potentially leading to *BRCA2* haploinsufficiency because although the splicing efficiency of this variant (both in the minigene assay and in patient RNA) is similar to that of the borderline c.316+6T>C noncoding variant, the c.316G>A transition: (i) produces a Gly>Arg missense change at a highly conserved amino acid position (Supplementary Fig. S17) in the residual *BRCA2* FL transcripts, and (ii) has been identified in *trans* of *BRCA2* c.2806_2809del [p.(Ala938Profs*21), paternal allele] in a FA patient, which is suggestive of a disease-causing hypomorphic variant.

To test this hypothesis, we then determined the functional consequences of c.316G>A (p.Gly106Arg) in the mESC assay. As shown in **Table 1**, c.316G>A lead to a drastic reduction of the number of HAT-resistant mESC colonies and a severe hypersensitivity to various DNA-damaging agents as compared with WT and to c.68-7T>A, strongly indicating an impairment of *BRCA2* function. Importantly, the complementation phenotype and degree of sensitivity to DNA-damaging agents were similar to those observed for c.316+6T>G and c.316+6T>A (**Table 1**; Supplementary Figs. S13 and S14) revealing that indeed c.316G>A (p.Gly106Arg) causes *BRCA2* haploinsufficiency but not total loss-of-function. Our results suggest that c.316G>A (Gly106Arg) is a hypomorphic allele that leads to *BRCA2* haploinsufficiency because of a negative impact both on *BRCA2e3* splicing and on FL protein function.

Discussion

Determining the pathogenicity of leaky *BRCA2* variants remains a major challenge in medical cancer genetics. To our knowledge, only one leaky *BRCA2* variant (c.68-7T>A) has been thoroughly assessed for its implication in HBOC (19). This variant has been classified as neutral by multifactorial analysis while all remaining *BRCA2* leaky variants linger as VUS until further evidence is collected (11, 19, 32). By using *BRCA2*e3 as a model system and complementary functional assays, we provide the first calibration of *BRCA2e3* spliceogenicity and an estimation of *BRCA2* mRNA-based haploinsufficiency, both of which contribute to the interpretation of leaky *BRCA2* variants. In addition, our study identified a plethora of new spliceogenic *BRCA2e3* variants.

To date, only 17 SNVs in/near *BRCA2*e3 (10 exonic and 7 intronic) have been reported as causing aberrant splicing, all shown to increase Δ3 (11, 12, 19, 27, 28, 32, 35, 38, 39). Our minigene results confirmed 15 of those initial findings (only 2 of the known spliceogenic variants being absent from our study) and uncovered 49 new splicing mutations (37 exonic, 10 intronic, and 2 at the exon–intron border) bringing the number of *BRCA2*e3 spliceogenic variants to a total of 66, most affecting potential SREs. Importantly, the vast majority of the detected splicing defects were leaky (54 of 64 spliceogenic variants), 45 being less drastic than the splicing anomaly caused by c.316+5G>C, but stronger than that observed for the neutral variant c.68-7T>A, which implied that they remained as of unknown significance. These observations suggest that variant-induced leaky splicing defects are prevalent in *BRCA2e3* and that additional analyses are warranted for accurate assessment of their pathogenicity. Still, among the 49 newly identified spliceogenic variants, 4 caused major loss of *BRCA2*e3 in the minigene assay similar to what was observed for c.316+5G>C. These variants (c.316+1G>A, c.316+1G>C, c.316+3A>C, and c.316+4_316+6delinsCGA) can thus be classified as pathogenic without further evidence (12). Moreover, we could also immediately classify 34 noncoding variants as neutral because they either had no impact on splicing in the minigene assay or induced a minor decrease in FL transcripts (equal or milder than c.68-7T>A).

To evaluate the biological significance of leaky splicing defects caused by *BRCA2e3* VUS, we next used a mESC-based assay known to reliably predict the pathogenicity of *BRCA2* variants (30, 31, 35, 40). We found that this assay recapitulates the normal alternative splicing of *BRCA2*e3 as well as variant-induced partial splicing defects. Indeed, although *BRCA2* Δ3 levels were somewhat variable in our complementary approaches probably due to different genomic environments, tissue-specific alternative splicing patterns and/or other experimental specificities, we demonstrated a high concordance in splicing phenotypes between the mESC assay and both minigene and patient RNA analysis. Moreover, data on mESC viability and sensitivity to DNA-damaging agents were concordant with the clinical classifications of c.68-7T>A and c.316+5G>C. By testing selected spliceogenic *BRCA2e3* VUS in the mESC assay, we were able to redefine cut-off

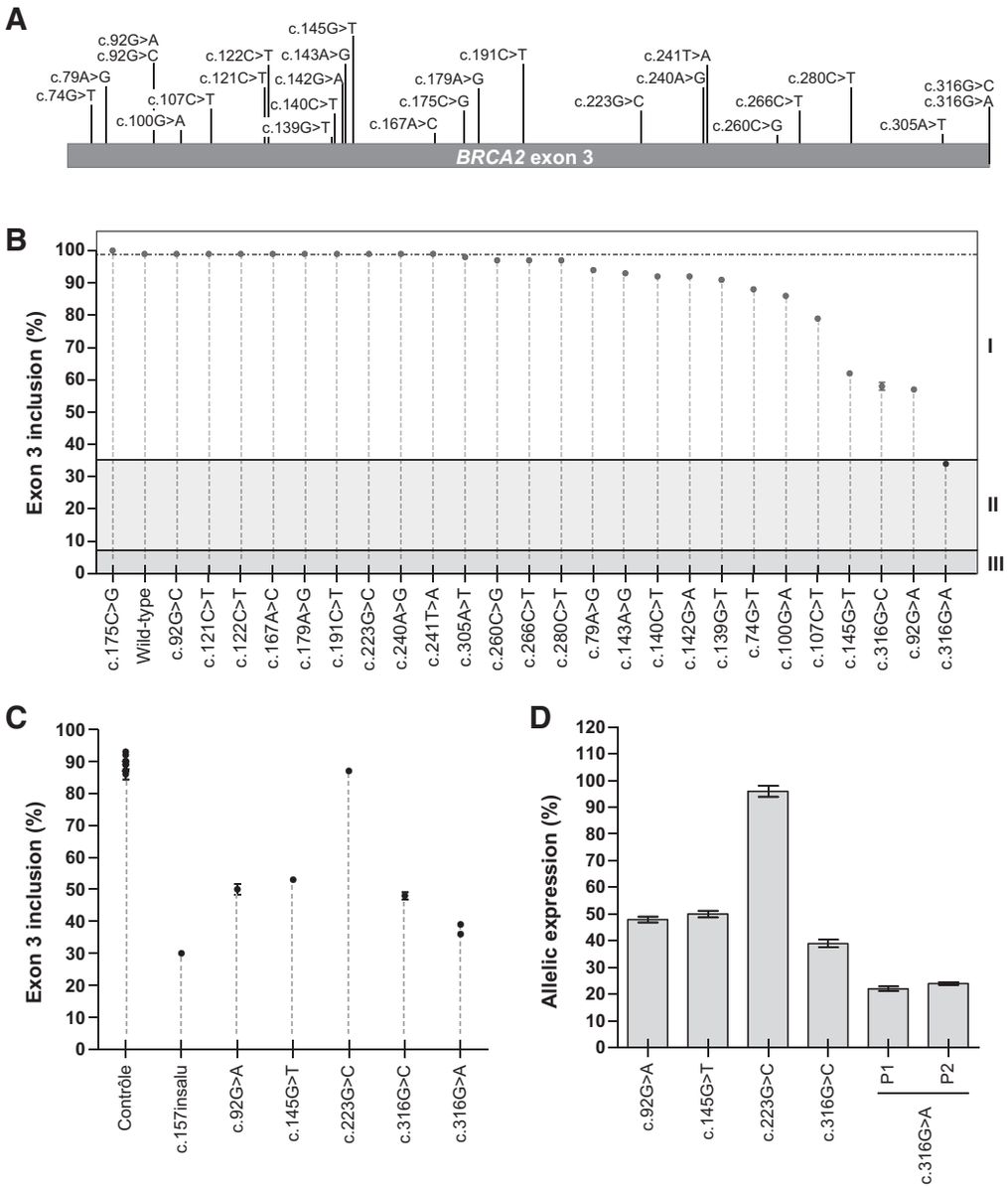

Figure 4.

RNA splicing impact of variants of unknown significance mapping to *BRCA2* exon 3. **A,** Distribution of the 26 selected coding variants within *BRCA2* exon 3. The diagram shows the relative position and identity of each variant within *BRCA2*e3 or its flanking intronic regions. **B,** Impact of *BRCA2* exon 3 variants on splicing observed in pCAS2-based minigene assays. Wild-type and mutant pCAS2-*BRCA2*-e3 minigene constructs were transiently expressed in HeLa cells. The splicing patterns of the RNA produced from the different minigenes were then analyzed by semiquantitative fluorescent RT-PCR, followed by capillary electrophoresis. Results represent the mean of exon 3 inclusion (FL) level of three independent transfection experiments. Error bars, SEM values. Dashed line, the level of FL produced by the WT minigene. Solid lines, FL levels that discriminate different classes of variants based on the splicing pattern of pCAS2-BRCA2e3 minigenes (c.316+6T>C and c.316+5G>C) and taking into account results from the mESC complementation assay shown in **Fig. 3:** likely neutral (**I**), of unknown clinical significance (**II**) and pathogenic variants (**III**). **C,** *BRCA2* exon 3 splicing patterns assessed in patient-derived samples. The *BRCA2*e3 splicing patterns in patient-derived RNA samples were monitored by semiquantitative fluorescent RT-PCR by using primers located in exons 2 and 5, and compared with those from healthy donors (controls). The levels of exon inclusion (FL) refer to the amount of full-length transcripts (containing exon 3) relative to the total amount of transcripts (with and without exon 3) and are representative of three independent experiments. Error bars, SEM values. **D,** Allele-specific expression of transcripts including *BRCA2* exon 3 measured by SNaPshot analysis in patient-derived samples. Genomic segment (gDNA) and complementary DNA (cDNA) containing *BRCA2*e3 were amplified in parallel using specific primers (gray arrows) and the SNaPshot quantitative primer extension assay was then performed with a variant-specific primer (black arrow) targeting the sequence immediately upstream the *BRCA2*e3 variant (star). Allele-specific expression levels, representing the relative contribution of the variant allele to the expression of full-length (FL) *BRCA2* transcripts as compared with WT (% of WT), were measured by normalization of the cDNA peak area ratio (variant/WT) to the corresponding gDNA peak area ratio (variant/WT). Results are representative of three independent experiments. Error bars, SEM values.

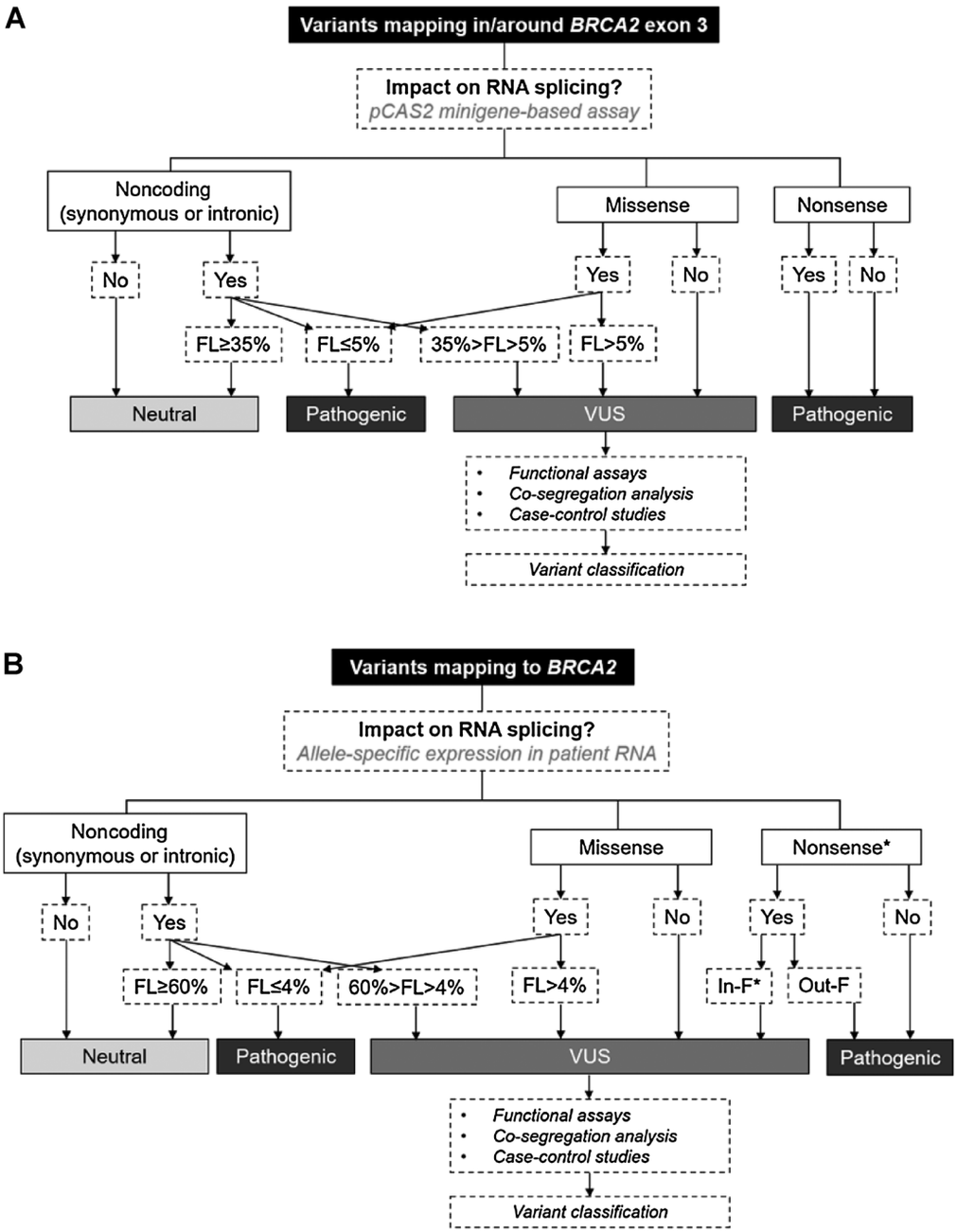

Figure 5.

Flowcharts describing the interest of RNA splicing assays and level of expression of *BRCA2* FL transcripts for classification of *BRCA2* VUS. **A,** Extreme decision thresholds for *BRCA2e3* variants based on data from pCAS2-BRCA2e3 minigene splicing assays and mESC complementation/survival results, notably on c.316+6T>C and c.316+5G>C (35% FL and 5% FL thresholds, respectively). **B,** Conservative decision thresholds for *BRCA2e3* variants, as well as for variants mapping outside *BRCA2e3*, based on data from ASE analysis (Supplementary Table S1). The 60% FL threshold derives from ASE results obtained with c.231T>G carriers. The 4% FL threshold was extrapolated from the c.316+5G>C minigene results by taking into account an adjustment factor of 0.77, which was determined by comparing minigene data with the ASE values obtained with exonic variants (Supplementary Table S1). These classification charts are not valid for variants inducing the production of transcripts containing in-frame indels that can lead to the synthesis of potentially/partially functional proteins. Nonsense*, nonsense variants outside the last exon of the gene; FL, full-length reference transcripts containing *BRCA2e3* (NM_000059.3); In-F*, in-frame RNA splicing alterations not affecting essential functional domains of the BRCA2 protein; Out-F, out-of-frame RNA splicing alterations resulting in frameshift modifications of *BRCA2* transcripts.

values, extrapolated from *BRCA2e3* splicing efficiencies, meant for improving variant interpretation (**Fig. 5A** and **B**). These thresholds allowed us to classify the 100 variants in our dataset as follows: 59 as neutral, 11 as pathogenic, and 30 as VUS (Supplementary Table S1). Our data suggests that noncoding *BRCA2e3* variants producing at least 27% FL transcripts in the mESC assay as compared with WT (or 35% in the minigene assay) can be considered neutral as they are expected to fully complement the loss of *BRCA2* in mESCs as seen for c.316+6T>C. A more conservative approach would be to take into account, as threshold for neutrality, the fraction of variant-expressed FL transcripts observed for c.231T>G (a minimum of 68%, 70%, or ∼60% FL in mESC, minigene or patients' RNA assays, respectively, as compared with WT) given that this is clearly a nonpathogenic variant. Indeed, our results indicate, for the first time, that *BRCA2* tumor suppressor activity tolerates a substantial reduction in FL expression from one allele independently of the synthesis of alternatively spliced functional transcripts. Interestingly, certain *BRCA1* and *BRCA2* variants responsible for drastic FL losses were recently reported as not being necessarily associated with high cancer risk or total loss-of-function (41, 42). However, in these cases, alternatively spliced transcripts leading to the production of potentially or partially functional isoforms (*BRCA1* Δ9, 10, or *BRCA2* Δ12, respectively) were generated, suggesting a rescue mechanism underlying the preserved BRCA function.

A window of uncertainty prevails for variants showing hypomorphic phenotypes in the mESC assay such as c.316+6T>A and c.316+6T>G that reduce FL transcripts to approximate;y15% WT in mESC (∼25% WT in the minigene assay). It is possible that these variants confer moderate risks of breast/ovarian cancer as shown for *BRCA1* c.5096G>A/p.Arg1699Gln and *BRCA2* c.9104A>C/p.Tyr3035Ser (43–45) or are associated with lower penetrance (45). Noncoding spliceogenic variants with incomplete penetrance and/or variable degrees of disease expressivity have already been described in other cancer predisposition genes such as *RB1* (46), *PMS2* (47), and *VHL* (48). Possibly such variability also exists within the spectra of *BRCA2* variants.

Further studies will be essential for illuminating genotype–phenotype correlations of spliceogenic *BRCA2* VUS identified as leaky in this and other studies. Given the rarity of most of these variants, informative studies will more likely stem from international collaborative efforts, such as those conducted by the ENIGMA consortium (49), allowing the collection of data on large number of patients and their families as well as to perform case–control genotyping analysis to accurately estimate cancer risks conferred by individual variants. Finally, because only minimal amounts of FL transcripts seem to be required for sufficient *BRCA2* function, our study may pave the way for the development of new cancer prevention strategies based on RNA splicing correction in patients carrying *BRCA2* splicing variants, according to the paradigm of spinal muscular atrophy (50).

Disclosure of Potential Conflicts of Interest

H. Tubeuf reports personal fees and nonfinancial support from Interactive Biosoftware [CIFRE PhD fellowship (#2015/0335)], grants from Groupement des Entreprises Françaises dans la Lutte contre le Cancer (Gefluc; Translational research grant), Fédération Hospitalo-Universitaire (FHU) Normandy Centre for Genomic and Personalized Medicine (NGP; translational research grant), European Union and Region Normandie (translational research grant), French National Cancer Institute and the Direction Générale de l'Offre des Soins (INCa/DGOS; translational research grant), European Regional Development Fund (ERDF; translational research grant); personal fees from EMBO (short-term fellowship #3436), Cancéropôle Nord-Ouest (short-term fellowship), and OpenHealth Institute during the conduct of the study. G. Castelain reports grants from French National Cancer Institute and the Direction Générale de l'Offre des Soins (INCa/DGOS), Groupement des Entreprises Françaises dans la Lutte contre le Cancer (Gefluc), and other from Fédération Hospitalo-Universitaire (FHU) Normandy Centre for Genomic and Personalized Medicine (NGP; financial support to Inserm U1245) and other from European Union and Region Normandie (financial support to Inserm U1245) during the conduct of the study; and H. Tubeuf was funded by a CIFRE PhD fellowship (#2015/0335) from the French Association Nationale de la Recherche et de la Technologie (ANRT) in the context of a public-private partnership between INSERM and Interactive Biosoftware. L. Meulemans reports grants from French National Cancer Institute and the Direction Générale de l'Offre des Soins (INCa/DGOS), grants from Groupement des Entreprises Françaises dans la Lutte contre le Cancer (Gefluc), other from Fédération Hospitalo-Universitaire (FHU) Normandy Centre for Genomic and Personalized Medicine (NGP; financial support to Inserm U1245), and other from European Union and Region Normandie (financial support to Inserm U1245) during the conduct of the study; and H. Tubeuf was funded by a CIFRE PhD fellowship (#2015/0335) from the French Association Nationale de la Recherche et de la Technologie (ANRT) in the context of a public-private partnership between INSERM and Interactive Biosoftware. P. Pujol reports grants and personal fees from Astrazeneca, Pfizer; personal fees from MSD and Exact Sciences outside the submitted work. F. Vaz reports other from Astrazeneca (collaborated with BRCA testing for observational study) outside the submitted work. C. Colas reports personal fees from AstraZeneca outside the submitted work. P. Gaildrat reports grants from French National Cancer Institute and the Direction Générale de l'Offre des Soins (INCa/DGOS), Groupement des Entreprises Françaises dans la Lutte contre le Cancer (Gefluc), other from Fédération Hospitalo-Universitaire (FHU) Normandy Centre for Genomic and Personalized Medicine (NGP; financial support to Inserm U1245), and other from European Union and Region Normandie (financial support to Inserm U1245) during the conduct of the study; and H. Tubeuf was funded by a CIFRE PhD fellowship (#2015/0335) from the French Association Nationale de la Recherche et de la Technologie (ANRT) in the context of a public-private partnership between INSERM and Interactive Biosoftware. A. Martins reports grants from French National Cancer Institute and the Direction Générale de l'Offre des Soins (INCa/DGOS), Groupement des Entreprises Françaises dans la Lutte contre le Cancer (Gefluc), other from Fédération Hospitalo-Universitaire (FHU) Normandy Centre for Genomic and Personalized Medicine (NGP; financial support to Inserm U1245), and other from European Union and Region Normandie (financial support to Inserm U1245) during the conduct of the study; and H. Tubeuf was funded by a CIFRE PhD fellowship (#2015/0335) from the French Association Nationale de la Recherche et de la Technologie (ANRT) in the context of a public-private partnership between INSERM and Interactive Biosoftware. No potential conflicts of interest were disclosed by the other authors.

Authors' Contributions

H. Tubeuf: Conceptualization, software, formal analysis, funding acquisition, validation, investigation, visualization, methodology, writing-original draft, writing-review and editing. **S.M. Caputo:** Resources, funding acquisition, investigation, writing-review and editing. **T. Sullivan:** Investigation. **J. Rondeaux:** Investigation. **S. Krieger:** Resources, writing-review and editing. **V. Caux-Moncoutier:** Resources. **J. Hauchard:** Investigation. **G. Castelain:** Investigation. **A. Fiévet:** Resources. **L. Meulemans:** Investigation. **F. Révillion:** Resources. **M. Léoné:** Resources. **N. Boutry-Kryza:** Resources. **C. Delnatte:** Resources. **M. Guillaud-Bataille:** Resources. **L. Cleveland:** Investigation. **S. Reid:** Investigation. **E. Southon:** Investigation. **O. Soukarieh:** Investigation. **A. Drouet:** Investigation. **D. Di Giacomo:** Investigation. **M. Vezain:** Investigation. **F. Bonnet-Dorion:** Resources. **V. Bourdon:** Resources. **H. Larbre:** Resources. **D. Muller:** Resources. **P. Pujol:** Resources. **F. Vaz:** Resources. **S. Audebert-Bellanger:** Resources. **C. Colas:** Resources. **L. Venat-Bouvet:** Resources. **A.R. Solano:** Resources. **D. Stoppa-Lyonnet:** Resources, funding acquisition. **C. Houdayer:** Resources, writing-review and editing. **T. Frebourg:** Resources, funding acquisition, writing-review and editing. **P. Gaildrat:** Conceptualization, supervision, funding acquisition, validation, investigation, writing-original draft, writing-review and editing. **S.K. Sharan:** Resources, supervision, funding acquisition, validation, investigation, writing-review and editing. **A. Martins:** Conceptualization, supervision, funding acquisition, validation, investigation, visualization, methodology, writing-original draft, project administration, writing-review and editing, study design and direction.

Acknowledgments

This work was funded by a translational research grant from the French National Cancer Institute and the Direction Générale de l'Offre des Soins (INCa/DGOS, AAP/CFB/CI), by the OpenHealth Institute, the Groupement des

Entreprises Françaises dans la Lutte contre le Cancer (Gefluc), the Fédération Hospitalo-Universitaire (FHU) Normandy Centre for Genomic and Personalized Medicine (NGP), the European Union and Region Normandie as well as by the Intramural Research Program from the Center for Cancer Research of the NCI, NIH. Europe gets involved in Normandie with European Regional Development Fund (ERDF). H. Tubeuf was funded by a CIFRE PhD fellowship (#2015/0335) from the French Association Nationale de la Recherche et de la Technologie (ANRT) in the context of a public–private partnership between INSERM and Interactive Biosoftware and by two short-term fellowship from EMBO (#3436) and Cancéropôle Nord-Ouest. J. Hauchard and G. Castelain were sponsored by the French INCa. The COVAR study is supported by the French Ligue contre le cancer and INCA BCB (2013-1-BCB-01-ICH-1) and by the GENETICANCER and « Cercle de l'Olympe ». We thank Sabine Tourneur (Inserm U1245, Rouen, France) for technical assistance.

The costs of publication of this article were defrayed in part by the payment of page charges. This article must therefore be hereby marked *advertisement* in accordance with 18 U.S.C. Section 1734 solely to indicate this fact.

Received March 31, 2020; revised May 14, 2020; accepted July 2, 2020; published first July 8, 2020.

References

1. Cline MS, Liao RG, Parsons MT, Paten B, Alquaddoomi F, Antoniou A, et al. BRCA Challenge: BRCA Exchange as a global resource for variants in BRCA1 and BRCA2. PLoS Genet 2018;14:e1007752.
2. Kuchenbaecker KB, Hopper JL, Barnes DR, Phillips K-A, Mooij TM, Roos-Blom M-J, et al. Risks of breast, ovarian, and contralateral breast cancer for BRCA1 and BRCA2 mutation carriers. JAMA 2017;317:2402–16.
3. Mersch J, Jackson MA, Park M, Nebgen D, Peterson SK, Singletary C, et al. Cancers associated with BRCA1 and BRCA2 mutations other than breast and ovarian. Cancer 2015;121:269–75.
4. Niraj J, Färkkilä A, D'Andrea AD. The fanconi anemia pathway in cancer. Annu Rev Cancer Biol 2019;3:457–78.
5. Caputo S, Benboudjema L, Sinilnikova O, Rouleau E, Béroud C, Lidereau R, et al. Description and analysis of genetic variants in French hereditary breast and ovarian cancer families recorded in the UMD-BRCA1/BRCA2 databases. Nucleic Acids Res 2012;40:D992–1002.
6. Landrum MJ, Lee JM, Riley GR, Jang W, Rubinstein WS, Church DM, et al. ClinVar: public archive of relationships among sequence variation and human phenotype. Nucleic Acids Res 2014;42:D980–5.
7. Eccles DM, Mitchell G, Monteiro ANA, Schmutzler R, Couch FJ, Spurdle AB, et al. BRCA1 and BRCA2 genetic testing-pitfalls and recommendations for managing variants of uncertain clinical significance. Ann Oncol 2015;26: 2057–65.
8. Lindor NM, Goldgar DE, Tavtigian SV, Plon SE, Couch FJ. BRCA1/2 sequence variants of uncertain significance: a primer for providers to assist in discussions and in medical management. Oncologist 2013;18:518–24.
9. Starita LM, Ahituv N, Dunham MJ, Kitzman JO, Roth FP, Seelig G, et al. Variant interpretation: functional assays to the rescue. Am J Hum Genet 2017;101: 315–25.
10. Cartegni L, Chew SL, Krainer AR. Listening to silence and understanding nonsense: exonic mutations that affect splicing. Nat Rev Genet 2002;3:285–98.
11. Bonnet C, Krieger S, Vezain M, Rousselin A, Tournier I, Martins A, et al. Screening BRCA1 and BRCA2 unclassified variants for splicing mutations using reverse transcription PCR on patient RNA and an ex vivo assay based on a splicing reporter minigene. J Med Genet 2008;45:438–46.
12. Caputo SM, Léone M, Damiola F, Ehlen A, Carreira A, Gaidrat P, et al. Full in-frame exon 3 skipping of BRCA2 confers high risk of breast and/or ovarian cancer. Oncotarget 2018;9:17334–48.
13. Prakash R, Zhang Y, Feng W, Jasin M. Homologous recombination and human health: the roles of BRCA1, BRCA2, and associated proteins. Cold Spring Harb Perspect Biol 2015;7:a016600.
14. Martinez JS, Baldeyron C, Carreira A. Molding BRCA2 function through its interacting partners. Cell Cycle 2015;14:3389–95.
15. Muller D, Rouleau E, Schultz I, Caputo S, Lefol C, Bièche I, et al. An entire exon 3 germ-line rearrangement in the BRCA2 gene: pathogenic relevance of exon 3 deletion in breast cancer predisposition. BMC Med Genet 2011;12:121.
16. Zou JP, Hirose Y, Siddique H, Rao VN, Reddy ES. Structure and expression of variant BRCA2a lacking the transactivation domain. Oncol Rep 1999;6:437–40.
17. Davy G, Rousselin A, Goardon N, Castéra L, Harter V, Legros A, et al. Detecting splicing patterns in genes involved in hereditary breast and ovarian cancer. Eur J Hum Genet 2017;25:1147–54.
18. Fackenthal JD, Yoshimatsu T, Zhang B, de Garibay GR, Colombo M, De Vecchi G, et al. Naturally occurring BRCA2 alternative mRNA splicing events in clinically relevant samples. J Med Genet 2016;53:548–58.
19. Colombo M, Lòpez-Perolio I, Meeks HD, Caleca L, Parsons MT, Li H, et al. The BRCA2 c.68-7T >A variant is not pathogenic: a model for clinical calibration of spliceogenicity. Hum Mutat 2018;39:729–41.
20. Leman R, Gaildrat P, Le Gac G, Ka C, Fichou Y, Audrezet M-P, et al. Novel diagnostic tool for prediction of variant spliceogenicity derived from a set of 395 combined in silico/in vitro studies: an international collaborative effort. Nucleic Acids Res 2020;48:1600–1.
21. Ke S, Shang S, Kalachikov SM, Morozova I, Yu L, Russo JJ, et al. Quantitative evaluation of all hexamers as exonic splicing elements. Genome Res 2011;21: 1360–74.
22. Di Giacomo D, Gaildrat P, Abuli A, Abdat J, Frébourg T, Tosi M, et al. Functional analysis of a large set of BRCA2 exon 7 variants highlights the predictive value of hexamer scores in detecting alterations of exonic splicing regulatory elements. Hum Mutat 2013;34:1547–57.
23. Erkelenz S, Theiss S, Otte M, Widera M, Peter JO, Schaal H. Genomic HEXploring allows landscaping of novel potential splicing regulatory elements. Nucleic Acids Res 2014;42:10681–97.
24. Xiong HY, Alipanahi B, Lee LJ, Bretschneider H, Merico D, Yuen RKC, et al. RNA splicing. The human splicing code reveals new insights into the genetic determinants of disease. Science 2015;347:1254806.
25. Rosenberg AB, Patwardhan RP, Shendure J, Seelig G. Learning the sequence determinants of alternative splicing from millions of random sequences. Cell 2015;163:698–711.
26. Tubeuf H, Charbonnier C, Soukarieh O, Blavier A, Lefebvre A, Dauchel H, et al. Large-scale comparative evaluation of user-friendly tools for predicting variant-induced alterations of splicing regulatory elements.
27. Sanz DJ, Acedo A, Infante M, Durán M, Pérez-Cabornero L, Esteban-Cardeñosa E, et al. A high proportion of DNA variants of BRCA1 and BRCA2 is associated with aberrant splicing in breast/ovarian cancer patients. Clin Cancer Res 2010; 16:1957–67.
28. Fraile-Bethencourt E, Valenzuela-Palomo A, Díez-Gómez B, Goina E, Acedo A, Buratti E, et al. Mis-splicing in breast cancer: identification of pathogenic BRCA2 variants by systematic minigene assays. J Pathol 2019;248:409–20.
29. Soukarieh O, Gaildrat P, Hamieh M, Drouet A, Baert-Desurmont S, Frébourg T, et al. Exonic splicing mutations are more prevalent than currently estimated and can be predicted by using in silico tools. PLoS Genet 2016; 12:e1005756.
30. Kuznetsov SG, Chang S, Sharan SK. Functional analysis of human BRCA2 variants using a mouse embryonic stem cell-based assay. Methods Mol Biol 2010; 653:259–80.
31. Kuznetsov SG, Liu P, Sharan SK. Mouse embryonic stem cell-based functional assay to evaluate mutations in BRCA2. Nat Med 2008;14:875–81.
32. Théry JC, Krieger S, Gaildrat P, Révillion F, Buisine M-P, Killian A, et al. Contribution of bioinformatics predictions and functional splicing assays to the interpretation of unclassified variants of the BRCA genes. Eur J Hum Genet 2011; 19:1052–8.
33. Machado PM, Brandão RD, Cavaco BM, Eugénio J, Bento S, Nave M, et al. Screening for a BRCA2 rearrangement in high-risk breast/ovarian cancer families: evidence for a founder effect and analysis of the associated phenotypes. J Clin Oncol 2007;25:2027–34.
34. Montalban G, Bonache S, Moles-Fernández A, Gadea N, Tenés A, Torres-Esquius S, et al. Incorporation of semi-quantitative analysis of splicing alterations for the clinical interpretation of variants in BRCA1 and BRCA2 genes. Hum Mutat 2019;40:2296–317.
35. Mesman RLS, Calléja FMGR, Hendriks G, Morolli B, Misovic B, Devilee P, et al. The functional impact of variants of uncertain significance in BRCA2. Genet Med 2019;21:293–302.
36. Richards S, Aziz N, Bale S, Bick D, Das S, Gastier-Foster J, et al. Standards and guidelines for the interpretation of sequence variants: a joint consensus

recommendation of the American College of Medical Genetics and Genomics and the Association for Molecular Pathology. Genet Med 2015;17:405–24.
37. Spurdle AB, Healey S, Devereau A, Hogervorst FBL, Monteiro ANA, Nathanson KL, et al. ENIGMA–evidence-based network for the interpretation of germline mutant alleles: an international initiative to evaluate risk and clinical significance associated with sequence variation in BRCA1 and BRCA2 genes. Hum Mutat 2012;33:2–7.
38. Biswas K, Das R, Eggington JM, Qiao H, North SL, Stauffer S, et al. Functional evaluation of BRCA2 variants mapping to the PALB2-binding and C-terminal DNA-binding domains using a mouse ES cell-based assay. Hum Mol Genet 2012; 21:3993–4006.
39. Thomassen M, Blanco A, Montagna M, Hansen TVO, Pedersen IS, Gutiérrez-Enríquez S, et al. Characterization of BRCA1 and BRCA2 splicing variants: a collaborative report by ENIGMA consortium members. Breast Cancer Res Treat 2012;132:1009–23.
40. Hendriks G, Morolli B, Calléja FMGR, Plomp A, Mesman RLS, Meijers M, et al. An efficient pipeline for the generation and functional analysis of human BRCA2 variants of uncertain significance. Hum Mutat 2014;35:1382–91.
41. de la Hoya M, Soukarieh O, López-Perolio I, Vega A, Walker LC, van Ierland Y, et al. Combined genetic and splicing analysis of BRCA1 c.[594-2A>C; 641A>G] highlights the relevance of naturally occurring in-frame transcripts for developing disease gene variant classification algorithms. Hum Mol Genet 2016;25:2256–68.
42. Meulemans L, Mesman R, Caputo S, Krieger S, Guillaud-Bataille Guillaud-Bataille M, Caux-Moncoutier V. Skipping nonsense to maintain function: the paradigm of BRCA2 exon 12. Cancer Res 2020;80:1374–86.
43. Moghadasi S, Meeks HD, Vreeswijk MP, Janssen LA, Borg Å, Ehrencrona H, et al. The BRCA1 c. 5096G>A p.Arg1699Gln (R1699Q) intermediate risk variant: breast and ovarian cancer risk estimation and recommendations for clinical management from the ENIGMA consortium. J Med Genet 2018;55:15–20.
44. Shimelis H, Mesman RLS, Von Nicolai C, Ehlen A, Guidugli L, Martin C, et al. BRCA2 hypomorphic missense variants confer moderate risks of breast cancer. Cancer Res 2017;77:2789–99.
45. Spurdle AB, Whiley PJ, Thompson B, Feng B, Healey S, Brown MA, et al. BRCA1 R1699Q variant displaying ambiguous functional abrogation confers intermediate breast and ovarian cancer risk. J Med Genet 2012;49:525–32.
46. Valverde JR, Alonso J, Palacios I, Pestaña A. RB1 gene mutation up-date, a meta-analysis based on 932 reported mutations available in a searchable database. BMC Genet 2005;6:53.
47. Sjursen W, Bjørnevoll I, Engebretsen LF, Fjelland K, Halvorsen T, Myrvold HE. A homozygote splice site PMS2 mutation as cause of Turcot syndrome gives rise to two different abnormal transcripts. Fam Cancer 2009;8:179–86.
48. Sexton A, Rawlings L, McKavanagh G, Simons K, Winship I. A Novel von Hippel Lindau Gene Intronic Variant and Its Reclassification from VUS to Pathogenic: the Impact on a Large Family. J Genet Couns 2015;24:882–9.
49. Parsons MT, Tudini E, Li H, Hahnen E, Wappenschmidt B, Feliubadaló L, et al. Large scale multifactorial likelihood quantitative analysis of BRCA1 and BRCA2 variants: An ENIGMA resource to support clinical variant classification. Hum Mutat 2019;40:1557–78.
50. Ramdas S, Servais L. New treatments in spinal muscular atrophy: an overview of currently available data. Expert Opin Pharmacother 2020;21:307–15.